High Thermopower and Low Thermal Conductivity in Semiconducting Ternary K−Bi−Se Compounds. Synthesis and Properties of β-$K_2Bi_8Se_{13}$ and $K_{2.5}Bi_{8.5}Se_{14}$ and Their Sb Analogues

Duck-Young Chung,[†] Kyoung-Shin Choi,[†] Lykourgos Iordanidis,[†] Jon L. Schindler,[‡] Paul W. Brazis,[‡] Carl R. Kannewurf,[‡] Baoxing Chen,[§] Siqing Hu,[§] Ctirad Uher,[§] and Mercouri G. Kanatzidis*[,†]

Department of Chemistry and Center for Fundamental Materials Research, Michigan State University, East Lansing, Michigan 48824; Department of Electrical and Computer Engineering, Northwestern University, Evanston, Illinois 60208; and Department of Physics, University of Michigan, Ann Arbor, Michigan 48109

Received May 30, 1997[⊗]

β-$K_2Bi_8Se_{13}$ (**I**), $K_2Sb_8Se_{13}$ (**II**), $K_{2.5}Bi_{8.5}Se_{14}$ (**III**), and $K_{2.5}Sb_{8.5}Se_{14}$ (**IV**) were synthesized by a molten flux method. The black needles of compound **I** were formed at 600 °C and crystallized in the monoclinic $P2_1/m$ space group (No. 11) with $a = 17.492(3)$ Å, $b = 4.205(1)$ Å, $c = 18.461(4)$ Å, $\beta = 90.49(2)°$. The final $R/R_w = 6.7/5.7\%$. Compound **II** is isostructural to **I**. Both **I** and **II** are isostructural with $K_2Bi_8S_{13}$ which is composed of NaCl-, Bi_2Te_3-, and CdI_2-type units connecting to form K^+-filled channels. The thin black needles of **III** and **IV** obtained at 530 °C crystallize in the same space group $P2_1/m$ with $a = 17.534(4)$ Å, $b = 4.206(1)$ Å, $c = 21.387(5)$ Å, $\beta = 109.65(2)°$ and $a = 17.265(3)$ Å, $b = 4.0801(9)$ Å, $c = 21.280(3)$ Å, $\beta = 109.31(1)°$, respectively. The final $R/R_w = 6.3/8.3\%$ and $5.1/3.6\%$. Compounds **III** and **IV** are isostructural and potassium and bismuth/antimony atoms are disordered over two crystallographic sites. The structure type is very closely related to that of **I**. Electrical conductivity and thermopower measurements show semiconductor behavior with ∼250 S/cm and ∼−200 μV/K for a single crystal of **I** and ∼150 S/cm and ∼−100 μV/K for a polycrystalline ingot of **III** at room temperature. The effect of vaccum annealing on these compounds is explored. The optical bandgaps of all compounds were determined to be 0.59, 0.78, 0.56, and 0.82 eV, respectively. The thermal conductivities of melt-grown polycrystalline ingots of **I** and **III** are reported.

Introduction

Since the solid solutions of $Bi_{2-x}Sb_xTe_{3-y}Se_y$[1] were established as the leading materials available for near-room-temperature thermoelectric applications, there have been continuing efforts to find better thermoelectric materials. The challenge lies in achieving simultaneously high electrical conductivity, high thermoelectric power, and low thermal conductivity. These properties define the thermoelectric figure of merit $ZT = (S^2\sigma/\kappa)T$, where S is the thermopower, σ the electrical conductivity, κ the thermal conductivity, and T the temperature. All three of these properties are determined by the details of the electronic structure and scattering of charge carriers (electrons or holes) and thus are not independently controllable parameters. κ also has a contribution from lattice vibrations, κ_l, the phonon thermal conductivity. Thus $\kappa = \kappa_e + \kappa_l$, where κ_e is the carrier thermal conductivity. To date, most investigations were mainly focused on tuning[2] the composition of Bi_2Q_3 (Q = S, Se, Te) solid solutions, doping[3] Bi_2Q_3 with other heavy metals, and optimizing device design. We have initiated an exploratory synthesis program to identify new multinary phases with Bi and Sb with narrow bandgaps which may be suitable as thermoelectric materials. This work is based on the proposition that materials with more complex compositions and structures may have complex electronic structures which may give rise to high thermoelectric powers, according to the Mott formula below, and at the same time possess low thermal conductivities. The thermopower S is given by

$$S = \frac{\pi^2}{3}\frac{k^2T}{e}\frac{\mathrm{d}\ \ln\sigma(E)}{\mathrm{d}E}\Big|_{E=E_f}$$

where $\sigma(E)$ is the electrical conductivity determined as a function of band filling. The electronic conductivity $\sigma = \sigma(E)|_{E=E_f}$ where E_f is the Fermi energy. If the carrier

[†] Michigan State University.
[‡] Northwestern University.
[§] University of Michigan.
[⊗] Abstract published in *Advance ACS Abstracts,* October 15, 1997.

(1) (a) Jeon, H.-H.; Ha, H.-P.; Hyun, D.-B.; Shim, J.-D. *J. Phys. Chem. Solids* **1991**, *4*, 579−585. (b) Testardi, L. R.; Bierly, J. N. Jr.; Donahoe, F. J. *J. Phys. Chem. Solids* **1962**, *23*, 1209. (c) Champness, C. H.; Chiang, P. T.; Parekh, P. *Can. J. Phys.* **1965**, *43*, 653−659; (d) **1967**, *45*, 3611−3626.

(2) (a) Yim, W. M.; Fitzke, E. V. *J. Electrochem. Soc.* **1968**, *115*, 556−560. (b) Yim, W. M.; Fitzke, E. V.; Rosi, F. D. *J. Mater. Sci.* **1966**, *1*, 52−65. (c) Borkowski, K.; Przyluski, J. *Mater. Res. Bull.* **1987**, *22*, 381−387.

(3) (a) Chizhevskaya, S. N.; Shelimova, L. E. *Inorg. Mater.* **1995**, *31*, 1083−1095. (b) Horák, J.; Cermák, K.; Koudelka, L. *J. Phys. Chem. Solids* **1986**, *47*, 805−809. (c) Lostak, P.; Horák, J.; Koudelka, L. *Phys. Status Solidi* **1983**, *76*, k71−k75. (d) Zalar, S. M. *Adv. Energy Conv.* **1962**, *2*, 105−112.

S0897-4756(97)00397-9 CCC: $14.00

scattering is independent of energy, then $\sigma(E)$ is just proportional to the density of states at E. In the general case, S is a measure of the difference in $\sigma(E)$ above and below the Fermi surface—specifically through the logarithmic derivative of with respect to E, see the equation above. So by manipulating the energy dependence of $\sigma(E)$ one can control simultaneously σ and S.

From a solid-state chemistry perspective, an intriguing feature of Bi/Sb chemistry is the stereochemical localization of their ns^2 lone-pair electrons, and the influence this exerts on the structure type and the electronic structure, and consequently the electronic properties of the resulting compounds. In this sense, alkali or alkaline earth metals introduced into the Bi_2Q_3 lattices rearrange the octahedrally coordinated Bi/Sb elements often causing the group 15 element to exhibit varying degrees of ns^2 lone-pair stereochemical activity. In addition to the multitude of naturally occurring sulfosalt minerals, several synthetic ternary alkali or alkaline earth metal group 15 chalcogenides are known such as ABQ_2 (A = alkali metal; B = group 15 metal; Q = chalcogen),[4] $CsBi_3S_5$,[5] $RbBi_3S_5$,[6] $Cs_3Bi_7Se_{12}$,[7] α,β-$BaBi_2S_4$,[8] $Sr_4Bi_6Se_{13}$,[9] $BaBiSe_3$,[10] K_3SbSe_4,[11] $RbSb_3Se_5$,[12] $Cs_2Sb_4Se_8$,[13] $Cs_3Sb_5Se_9$,[14] $Ca_2Sb_2S_5$,[15] $Ba_8Sb_6S_{17}$,[16] and $Sr_3Sb_4S_9$,[17] which were prepared at high temperature by direct combination of the elements or alkali carbonates with Bi/Sb and S/Se.

We have recently contributed to this area of chemistry by reporting on the synthesis, structure and function of β,γ-$CsBiS_2$,[18] KBi_3S_5,[19] $KBi_{6.33}S_{10}$,[20] $K_2Bi_8S_{13}$,[20] α-$K_2Bi_8Se_{13}$,[18] $BaBiTe_3$,[21] $Cs_2Sb_4S_8$,[22] $CsSbS_6$,[22] $KThSb_2Se_6$,[23] and $BaLaBi_2Q_6$ (Q = S, Se)[23]. Some of these compounds have highly promising thermoelectric properties.[20,21] In a previous publication we reported that $K_2Bi_8S_{13}$ possesses significantly higher electrical conductivity ($\sim 10^2$ S/cm) at room temperature than that of its parent compound, Bi_2S_3,[24] and shows unusually high thermopower.[20] The Seebeck coefficient of $K_2Bi_8S_{13}$, however, differs greatly in samples of different preparation, which we think is due to the fact that in this compound there is occupancy disorder in some crystallographic sites between K^+ and Bi^{3+}. If the degree of disorder varies from sample to sample, it would make preparation of strictly identical samples difficult. In the hope of avoiding or minimizing the K/Bi disorder and better control over the electrical properties, we prepared the isostructural Se analogue of this compound. Furthermore, in going from the S to the heavier Se analogue, we expected the thermal conductivity to decrease substantially.

We report here the synthesis, physicochemical, spectroscopic, and structural characterization of the new compounds, β-$K_2Bi_8Se_{13}$, $K_2Sb_8Se_{13}$, $K_{2.5}Bi_{8.5}Se_{14}$, and $K_{2.5}Sb_{8.5}Se_{14}$. While β-$K_2Bi_8Se_{13}$ is isostructural with $K_2Bi_8S_{13}$, the isostructural $K_{2.5}Bi_{8.5}Se_{14}$ and $K_{2.5}Sb_{8.5}Se_{14}$ are different but with structural features similar to those of β-$K_2Bi_8Se_{13}$. The complete set of thermoelectric measurements: electrical conductivity, Seebeck coefficient and thermal conductivity, for β-$K_2Bi_8Se_{13}$ and $K_{2.5}Bi_{8.5}Se_{14}$ are reported over a wide temperature range. Compared with α-$K_2Bi_8Se_{13}$, which possesses a room-temperature electrical conductivity of 2 S/cm and a Seebeck coefficient ranging from −210 to −260 μV/K,[18] β-$K_2Bi_8Se_{13}$ shows an extraordinarily high electrical conductivity at room temperature while maintaining a high Seebeck coefficient (−200 μV/K).

Experimental Section

Reagents. Chemicals in this work were used as obtained: (i) bismuth powder, 99.999+ % purity, −100 mesh, Cerac, Milwaukee, WI, (ii) antimony metal, 99.999% purity, −325 mesh, Cerac Inc., Milwaukee, WI, (iii) selenium powder, 99.95% purity, −200 mesh, Cerac Inc., Milwaukee, WI, (iv) potassium metal, rod, 99.5% purity, Aldrich Chemical Co., Inc., Milwaukee, WI.

Synthesis. All manipulations were carried out under a dry nitrogen atmosphere in a Vacuum Atmospheres Dri-Lab glovebox. K_2Se was obtained by a stoichiometric reaction of elemental potassium and selenium in liquid NH_3.

*β-$K_2Bi_8Se_{13}$ (**I**).* A mixture of K_2Se (0.043 g, 0.274 mmol), elemental Bi (0.2 g, 0.957 mmol), and elemental Se (0.130 g, 1.646 mmol) was loaded into a carbon-coated quartz tube (9 mm diameter) and subsequently flame-sealed at a residual pressure of $<10^{-4}$ Torr. The mixture was heated to 600 °C over 24 h and kept there for 6 days, followed by slowly cooling to 200 °C at a rate of −4 °C/h and then to 50 °C in 12 h. Metallic black needles of β-$K_2Bi_8Se_{13}$ were obtained quantitatively by isolation in dimethylformamide (DMF) and washing with diethyl ether. A quantitative microprobe analysis with a SEM/EDS system was performed on several crystals to give an approximate ratio of $K_{1.8}Bi_{8.6}Se_{13}$.

*$K_2Sb_8Se_{13}$ (**II**).* A mixture of K_2Se (0.069 g, 0.439 mmol), elemental Sb (0.364 g, 2.99 mmol), and elemental Se (0.382 g, 4.84 mmol) was loaded into a Pyrex tube (9 mm diameter) and subsequently flame-sealed at a residual pressure of $<10^{-3}$ Torr.

(4) (a) Boon, J. W. *Recl. Trav. Chim. Pays-Bas* **1944**, *63*, 32. (b) Glemser, O.; Filcek, M. *Z. Anorg. Allg. Chem.* **1955**, 279, 321−323. (c) Gattow, G.; Zemann, J. *Z. Anorg. Allg. Chem.* **1955**, *279*, 324−327. (d) Voroshilov, Y. V.; Peresh, E. Y.; Golovei, M. I. *Inorg. Mater.* **1972**, *8*, 777−778.
(5) Kanischeva, A. S.; Mikhailov, J. N.; Lasarev, V. B.; Trippel, A. F. *Dokl. Akad. Nauk., SSSR (Kryst.)* **1980**, *252*, 96−99.
(6) Schmitz, D.; Bronger, W. *Z. Naturforsch.* **1974**, *29b*, 438−439.
(7) Cordier, G.; Schäfer, H.; Schwidetzky, C. *Rev. Chim. Miner.* **1985**, *22*, 676−683.
(8) Aurivillus, B. *Acta Chem. Scand.* **1983**, *A37*, 399−407.
(9) Cordier, G.; Schäfer, H.; Schwidetzky, C. *Rev. Chim. Miner.* **1985**, *22*, 631−638.
(10) Volk, K.; Cordier, G.; Cook, R.; Schäfer, H. *Z. Naturforsch.* **1980**, *35b*, 136−140.
(11) Eisenmann, B.; Zagler, R. *Z. Naturforsch.* **1989**, *44b*, 249−256.
(12) Sheldrick, W. S.; Häusler, H. J. *Z. Anorg. Allg. Chem.* **1988**, *557*, 98−104.
(13) Sheldrick, W. S.; Kaub, J. *Z. Anorg. Allg. Chem.* **1986**, *536*, 114−118.
(14) Sheldrick, W. S.; Häusler, H.-J. *Z. Anorg. Allg. Chem.* **1988**, *561*, 149−156.
(15) Cordier, G.; Schäfer, H. *Rev. Chim. Miner.* **1981**, *18*, 218−223.
(16) Dorrscheidt, W.; Schäfer, H. *Z. Naturforsch.* **1981**, *36B*, 410−414.
(17) Cordier, G.; Schwidetzky, C.; Schäfer, H. *Rev. Chim. Miner.* **1982**, *19*, 179−186.
(18) McCarthy, T. J.; Ngeyi, S.-P.; Liao, J.-H.; DeGroot, D.; Hogan, T.; Kannewurf, C. R.; Kanatzidis, M. G. *Chem. Mater.* **1993**, *5*, 331−340.
(19) McCarthy, T. J.; Tanzer, T. A.; Kanatzidis, M. G. *J. Am. Chem. Soc.* **1995**, *117*, 1294−1301.
(20) (a) Kanatzidis, M. G.; McCarthy, T. J.; Tanzer, T. A.; Chen, L.-H.; Iordanidis, L.; Hogan, T.; Kannewurf, C. R.; Uher, C.; Chen, B. *Chem. Mater.* **1996**, *8*, 1465−1474. (b) Kanatzidis, M. G.; McCarthy, T. J.; Tanzer, T. A.; Chen, L.-H.; Hogan, T.; Kannewurf, C. R.; Iordanidis, L. *Mater. Res. Soc. Symp. Proc.* **1996**, *410*, 37−43. (c) Chung, D.-Y.; Hogan, T.; Schindler, J.; Iordanidis, L.; Brazis, P.; Kannewurf, C. R.; Chen, B.; Uher, C.; Kanatzidis, M. G. *Mat. Res. Soc. Symp. Proc.* **1997**, *478*, 333−344.
(21) (a) Chung, D.-Y.; Jobic, S.; Hogan, T.; Kannewurf, C. R.; Brec, R.; Rouxel, J.; Kanatzidis, M. G. *J. Am. Chem. Soc.*, in press. (b) Chung, D.-Y.; Jobic, S.; Hogan, T.; Kannewurf, C. R.; Brec, R.; Rouxel, J.; Kanatzidis, M. G. *Mat. Res. Soc. Symp. Proc.* **1997**, *453*, 15−22.
(22) McCarthy, T. J.; Kanatzidis, M. G. *Inorg. Chem.* **1994**, *33*, 1205−1211.
(23) Choi, K.-S.; Iordanidis, L.; Chondroudis, K.; Kanatzidis, M. G. *Inorg. Chem.* **1997**, *36*, 3804−3805.
(24) (a) Gildart, L.; Kline, J. M.; Martox, D. M. *J. Phys. Chem. Solids* **1961**, *28*, 246. (b) Nayak, B. B.; Acharya, H. N. *J. Mater. Sci.* **1986**, *21*, 46.

The mixture was heated to 530 °C over 12 h and kept there for 5 days, followed by slowly cooling to 200 °C at a rate of −2 °C/h and then to 50 °C in 12 h. Thin black needles of $K_2Sb_8Se_{13}$ were obtained in quantitative yield by isolation in DMF. SEM/EDS analysis on several crystals showed the approximate ratio of $K_{1.9}Sb_{7.7}Se_{13}$.

*$K_{2.5}Bi_{8.5}Se_{14}$ (**III**).* A mixture of K_2Se (0.045 g, 0.286 mmol), elemental Bi (0.2 g, 0.957 mmol), and elemental Se (0.125 g, 1.583 mmol) was loaded into a Pyrex tube (9 mm diameter) and subsequently flame-sealed at a residual pressure of $<10^{-3}$ Torr. The mixture was heated to 530 °C over 12 h and kept there for 5 days, followed by slowly cooling to 200 °C at a rate of −2 °C/h and then to 50 °C in 12 h. Metallic black microneedles mixed with black powder were obtained by the isolation as above in DMF. Dried product was homogeneously ground and loaded into a quartz tube and sealed at $<10^{-4}$ Torr. After recrystallizing the mixture by melting at 750 °C, shiny lump of black needles of $K_{2.5}Bi_{8.5}Se_{14}$ was obtained in a pure state. SEM/EDS analysis on several crystals showed the approximate ratio of $K_{2.9}Bi_{9.0}Se_{14}$.

*$K_{2.5}Sb_{8.5}Se_{14}$ (**IV**).* A mixture of K_2Se (0.063 g, 0.40 mmol), elemental Sb (0.097 g, 0.80 mmol), and elemental Se (0.126 g, 1.60 mmol) was loaded into a Pyrex tube (9 mm diameter) and subsequently flame-sealed at a residual pressure of $<10^{-3}$ Torr. The mixture was heated to 530 °C over 12 h and kept there for 5 days, followed by slowly cooling to 200 °C at a rate of −2 °C/h and then to 50 °C in 12 h. Thin metallic black needles of $K_{2.5}Sb_{8.5}Se_{14}$ were obtained quantitatively by the isolation in DMF. SEM/EDS analysis on several crystals showed the approximate ratio of $K_{1.8}Sb_{8.9}Se_{14}$.

Physical Measurements. Electron Microscopy. Quantitative microprobe analyses of the compound were performed with a JEOL JSM-35C scanning electron microscope (SEM) equipped with a Tracor Northern energy-dispersive spectroscopy (EDS) detector. Data were acquired using an accelerating voltage of 20 kV and a 1 min accumulation time.

Differential Thermal Analysis. Differential thermal analysis (DTA) was performed with a computer-controlled Shimadzu DTA-50 thermal analyzer. The ground single crystals (~20 mg total mass) were sealed in quartz ampules under vacuum. A quartz ampule containing alumina of equal mass was sealed and placed on the reference side of the detector. The samples were heated to the desired temperature at 10 °C/min and then isothermed for 3 min followed by cooling at 10 °C/min to 100 °C and finally by rapid cooling to room temperature. The reported DTA temperature is the peak temperature. The DTA sample was examined by powder X-ray diffraction after the experiment.

Infrared Spectroscopy. Optical diffuse reflectance measurements were made on the finely ground sample at room temperature. The spectrum was recorded in the infrared region (6000−400 cm^{-1}) with the use of a Nicolet MAGNA-IR 750 Spectrometer equipped with a collector diffuse reflectance of Spectra-Tech. Inc. The measurement of diffuse reflectivity can be used to obtain values for the bandgap which agree rather well with the values obtained by absorption measurements from single crystals of the same material. Absorption (α/S) data were calculated from the reflectance data using the Kubelka−Munk function:[25] $\alpha/S = (1 - R)^2/2R$, where R is the reflectance at a given wavenumber, α is the absorption coefficient, and S is the scattering coefficient. The scattering coefficient has been shown to be practically wavenumber independent for particles larger than 5 μm, which is smaller than the particle size of the samples used here. The bandgap was determined as the intersection point between energy axis at the absorption offset and the line extrapolated from the linear portion of the absorption edge in a α/S vs E (eV) plot.

Solid-State UV/Vis Spectroscopy. Optical diffuse reflectance measurements were made at room temperature with a Shimadzu UV-3101 PC double-beam, double-monochromator spectrophotometer operating in the 200−2500 nm region. The instrument was equipped with an integrating sphere and controlled by a personal computer. The measurement of diffuse reflectivity can be used to obtain values for the bandgap which agree rather well with values obtained by absorption measurements on single crystals of the same material. The digitized spectra were processed using the Kaleidagraph software program. $BaSO_4$ powder was used as reference (100% reflectance). Absorption data were calculated from the reflectance data using the Kubelka−Munk function as above.

Charge-Transport and Thermal Conductivity Measurements. Dc electric conductivity and thermopower measurements were made on single crystals and polycrystalline compactions of the compound. Conductivity measurements were performed in the usual four-probe geometry with 60- and 25-μm gold wires used for the current and voltage electrodes, respectively. Measurements of the pellet cross-sectional area and voltage probe separation were made with a calibrated binocular microscope. Conductivity data were obtained with the computer-automated system described elsewhere.[18,26a] Thermoelectric power measurements were made by using a slow ac technique[18,26b] with 60 μm gold wires serving to support and conduct heat to the sample, and 10 μm wires to measure the voltage across the sample resulting from the applied temperature gradient. In both measurements, the gold electrodes were held in place on the sample with a conductive gold or silver paste.

Conductivity specimens were mounted on interchangeable sample holders, and thermopower specimens were mounted on a fixed sample holder/differential heater. Mounted samples were placed under vacuum ($\leq 10^{-3}$ Torr) and held at room temperature for 2−4 h to cure the gold contacts. For some variable-temperature runs, data (conductivity or thermopower) were acquired during both sample cooling and warming to check reversibility. The temperature drift rate during an experiment was kept below 1 K/min. For single crystal measurements several variable-temperature runs were carried out for each sample to assess the consistency of the measured properties.

The thermal conductivity of polycrystalline samples was measured using a steady-state method. Samples were attached to the cold tip of a variable-temperature cryostat with the aid of Stycast epoxy. A small strain-gauge resistor serving as a heater was glued to the other end of the sample. Small crossbars made of flattened 0.25 mm diameter copper wire were attached with a tiny amount of Stycast at two positions along the length of a cylindrical sample. The samples were grown as cylindrical polycrystalline ingots by a recrystallization from the melt inside quartz tubes. Because the samples of **III** decompose with time when molten (see discussion below), ingots from this compound were grown by rapid melting recrystallization procedure (<15 min) using an rf furnace. A pair of calibrated chromel−constantan differential thermocouples (25 μm diameter wires) was soldered to the copper crossbars to measure both the temperature difference ΔT and the temperature of the cold junction. Thermal conductivity was then determined from $\kappa = Ql/S\Delta T$, where Q is the power applied to the heater, l is the spacing between the crossbars, and S is the cross-sectional area of the sample. Measurements were carried out in a vacuum better than 10^{-6} Torr over the temperature range 4−300 K.

Crystallography. The compounds were examined by X-ray powder diffraction for the purpose of phase purity and identification. Accurate d_{hkl} spacings (Å) were obtained from the powder patterns recorded on a Rigaku Rotaflex powder X-ray diffractometer with Ni-filtered Cu Kα radiation operating at 45 kV and 100 mA. The data were collected at a rate of 0.4°/min.

The intensities of three standard reflections were checked every 150 reflections to monitor crystal and instrument stability during single-crystal X-ray data collection. The structures of all compounds were solved by direct methods using the SHELXS-86 software program. After empirical absorption corrections based on ψ scans, refinements with full-matrix least-squares techniques and Fourier synthesis calculations were carried out with the TEXSAN package of crystallographic programs.

(25) (a) Wendlandt, W. W.; Hecht, H. G. *Reflectance Spectroscopy*; Interscience Publishers: New York, 1966. (b) Kotüm, G. *Reflectance Spectroscopy*; Springer-Verlag: New York, 1969. (c) Tandon, S. P.; Gupta, J. P. *Phys. Status Solidi* **1970**, *38*, 363−367.

Structure Solution of β-$K_2Bi_8Se_{13}$. A single crystal of β-$K_2Bi_8Se_{13}$ with dimensions 0.02 × 0.08 × 0.26 mm was mounted on the tip of a glass fiber. The crystallographic data were collected at room temperature on a Rigaku AFC6S four-circle automated diffractometer equipped with a graphite-crystal monochromator. No significant decay was observed during the data collection period. The data were collected with the $\theta/2\theta$ scan technique. The unit-cell parameters were determined from a least-squares refinement using the 2θ angles of 15 carefully centered reflections in the $6 \le 2\theta \le 20°$ range. Eight Bi atoms, thirteen Se atoms, and two K atoms were located in mirror planes. After least-squares refinement, the isotropic temperature factor for Bi(8) was high at 7.7 Å^2 while the isotropic temperature factor for K(1) was negative at −0.8 Å^2 ($R/R_w = 10.2/9.7\%$). Refinement of the occupancies of Bi(8) and K(1) showed a large decrease for Bi(8) (0.335) and a large increase for K(1) (1.158). The ideal occupancy for both sites is 0.500. Since the coordination environment of the two sites is similar, a model with Bi and K disordered between the two sites was applied. Successive refinements using this model resulted in a formula of $K_{2.06}Bi_{7.94}Se_{13}$ where a additional +0.12 charge is needed for electroneutrality ($R/R_w = 8.8/8.5\%$). The occupancies were rounded off and fixed to $K_2Bi_8Se_{13}$ with no significant change in the R values. The atomic composition of the Bi-rich site is 62% Bi and 38% K while the opposite applies for the K-rich site. All atoms were refined anisotropically ($R/R_w = 7.8/6.8\%$). Averaging the data improved the R/R_w values 6.7/5.7%. As a check for Bi−K disorder in the K(2) site, the occupancy of the K(2) was refined and revealed no change, suggesting that this site is fully occupied by K.

Structure Solution of $K_{2.5}Bi_{8.5}Se_{14}$. A single crystal with dimensions 0.02 × 0.08 × 0.51 mm was mounted on a glass fiber and the crystallographic data were collected at room temperature on a Rigaku AFC6S diffractometer by the same procedure as above. Intensity data were collected using the $\theta/2\theta$ scan mode. The unit-cell parameters were determined from a least-squares refinement using the 2θ angles of 17 carefully centered reflections in the $8 \le 2\theta \le 28°$ range. An empirical absorption correction based on ψ scans was applied to the data. Eight Bi atoms, fourteen Se atoms, and three K atoms were found on mirror planes. After least-squares refinement, the isotropic temperature factors for K(1) and K(3) were negative at −1.01 and −0.90 Å^2 respectively ($R/R_w = 10.0/12.6\%$). The occupancies and temperature factors were refined to give values of 0.87/1.86 Å^2 for K(1) and 0.96/2.79 Å^2 for K(3) (full occupancy of a special position on mirror plane is 0.5) with $R/R_w = 9.3/11.1\%$. At a distance of 0.48 Å from K(3), there was a high electron density (23.09 e/Å^3) peak which behaved very well as a disordered Bi atom. This suggested that a structural model with K and Bi disordered over these two K sites seemed reasonable. Therefore, Bi(7) was assigned to be disordered with K(3) and Bi(5) disordered with K(1). Successive refinements, taking into account this model, resulted in reasonable occupancies and temperature factors which were 0.38/2.74 Å^2 for K(1), 0.12/2.74 Å^2 for Bi(5), 0.36/1.41 Å^2 for K(3), and 0.14/0.93 Å^2 for Bi(7) with $R/R_w = 7.5/9.5\%$ and thus a formula $K_{2.48}Bi_{8.52}Se_{14}$. The occupancies were rounded off and fixed to obtain electroneutrality. Least-squares refinement gave $K_{2.5}Bi_{8.5}Se_{14}$ with $R/R_w = 7.4/9.3\%$. A DIFABS correction was applied to the isotropically refined data ($R/R_w = 6.8/8.8\%$). All atoms except the disordered atoms were refined anisotropically ($R/R_w = 6.3/8.3\%$).

Structure Solution of $K_{2.5}Sb_{8.5}Se_{14}$. A single crystal with dimensions 0.09 × 0.13 × 0.26 mm was mounted on a glass fiber and the crystallographic data were collected at −140 °C on a Nicolet P3 diffractometer by the same procedure as above. Intensity data were collected using the $\theta/2\theta$ scan mode. The unit-cell parameters were determined from a least-squares refinement using the 2θ angles of 20 carefully centered reflections in the $8 \le 2\theta \le 25°$ range. An empirical absorption correction based on ψ scans was applied to the data. Eight Sb atoms, fourteen Se atoms, and three K atoms were found on mirror planes. In the same way as $K_{2.5}Bi_{8.5}Se_{14}$, a disordered model between Sb and K atoms was successfully adopted to improve the negative temperature factors of K(1) and K(3). Sb(5) and Sb(7) were assigned to electron density peaks near K(1) and K(3), respectively, to assume a positionally disordered model. Their final occupancies and temperature factors were 0.42/0.8 Å^2 for K(1), 0.08/0.8 Å^2 for Bi(5), 0.26/1.2 Å^2 for K(3), and 0.24/1.2 Å^2 for Bi(7) with a formula $K_{2.36}Sb_{8.64}Se_{14}$. The occupancies were fixed to $K_{2.5}Sb_{8.5}Se_{14}$ to obtain charge balance. After successive refinements, the isotropic temperature factors for Se(2), Se(4), and Se(6) were still very high as 5.9, 3.5, and 10.5 Å^2, indicating that these selenium atoms might be also disordered in this structure. The rotational axial photo along the a-axis showed a weak 2-fold superlattice which makes the a-axis parameter 34.530 Å. However, it was impossible to solve the structure as a supercell because of the very few and weak intensities of the superlattice peaks. Therefore, we proceeded with a disorder model. Each of these selenium atoms had significant electron density peaks in their proximity (<0.64 Å), which were assigned to Se(2′), Se(4′), and Se(6′), respectively. After this procedure, the isotropic temperature factors of the original selenium atoms dropped to reasonable values. Their final occupancies and temperature factors were 0.31/1.4 Å^2 for Se(2), 0.19/1.4 Å^2 for Se(2′), 0.35/1.8 Å^2 for Se(4), 0.15/1.8 Å^2 for Se(4′), 0.24/0.9 Å^2 for Se(6), and 0.26/0.9 Å^2 for Se(6′). All atoms were refined anisotropically except the disordered atoms ($R/R_w = 5.1/3.6\%$).

Table 1. Summary of Crystallographic Data and Structural Analysis for β-$K_2Bi_8Se_{13}$, $K_{2.5}Bi_{8.5}Se_{14}$, and $K_{2.5}Sb_{8.5}Se_{14}$

formula	β-$K_2Bi_8Se_{13}$	$K_{2.5}Bi_{8.5}Se_{14}$	$K_{2.5}Sb_{8.5}Se_{14}$
formula weight	2776.52	2979.52	2238.06
crystal habit	black needle	black needle	black needle
space group	$P2_1/m$ (No. 11)	$P2_1/m$ (No. 11)	$P2_1/m$ (No. 11)
a, Å	17.492(3)	17.535(4)	17.265(3)
b, Å	4.205(1)	4.206(2)	4.080(1)
c, Å	18.461(4)	21.387(5)	21.278(4)
β, deg	90.49(2)	109.65(2)	109.31(1)
Z; V, Å^3	4; 1357.8(5)	4; 1486(2)	4; 1414.4(5)
D_{calc}, g/cm^{-3}	6.791	6.661	6.191
temp, K	298	298	133
λ(Mo Kα), Å	0.71073	0.71073	0.71073
μ(Mo Kα)/cm^{-1}	692.79	673.54	304.38
scan mode	$\theta-2\theta$	$\theta-2\theta$	$\theta-2\theta$
$2\theta_{max}$, deg	50.0	45.0	50.0
total data measd	4906	2356	4898
total unique data	3570	2270	2447
data with $I > 3\sigma(I)$	1191	1202	762
no. of variables	139	148	162
final R^a/R_w,^{b} %	6.7/5.7	6.3/8.3	5.1/3.6
goodness of fit	2.6	2.6	1.9

^{a} $R = \sum||F_o| - |F_c||/\sum|F_o|$. ^{b} $R_w = \{\sum w(|F_o| - |F_c|)^2/\sum w|F_o|^2\}^{1/2}$.

Table 1 shows the crystal data and the details of the structure analysis for all compounds. The fractional coordinates and the equivalent atomic displacement parameters (B_{eq}) of all the atoms with their estimated standard deviations are given in Tables 2−4. Selected bond lengths and angles in the compounds are summarized in Tables 5−10.

Results and Discussion

Synthesis, Thermal Analysis, and Spectroscopy. In comparison with $K_2Bi_8S_{13}$, which is prepared only by direct combination of Bi_2S_3 and K_2S at 750 °C, the synthesis of the isomorphous phase β-$K_2Bi_8Se_{13}$ can be accomplished both by a direct combination reaction at 600 °C and by a flux reaction of Bi and K_2Se/Se at 600 °C followed by isolation in DMF. The α-$K_2Bi_8Se_{13}$ can be obtained by a relatively wide range of molar ratio of Bi and K_2Se/Se between 330 and 370 °C.[18] Our investigation in the K/Bi/Se system under K_2Se_x flux conditions suggests that α-$K_2Bi_8Se_{13}$ and β-$K_2Bi_8Se_{13}$ are stable phases within a limited temperature window of stability but with a relatively wide range of flux composition. The α-form, which only forms in a flux, is surely the kinetically stabilized phase, while β-$K_2Bi_8Se_{13}$ is the thermodynamically more stable phase.

Table 2. Fractional Atomic Coordinates and Equivalent Atomic Displacement Parameter (B_{eq}) Values for β-$K_2Bi_8Se_{13}$ with Estimated Standard Deviations in Parentheses

atom	*x*	*y*	*z*	B_{eq},[a] Å^2
Bi(1)	0.9192(2)	1/4	0.0785(3)	1.45(9)
Bi(2)	0.1729(2)	−3/4	0.1239(3)	1.65(9)
Bi(3)	0.3273(2)	−1/4	−0.0184(2)	1.36(9)
Bi(4)	0.8938(2)	−3/4	0.4761(3)	1.9(1)
Bi(5)	0.6954(2)	−1/4	0.4509(2)	1.45(9)
Bi(6)	1.0145(2)	−1/4	0.2524(2)	1.7(1)
Bi(7)	0.4939(2)	−3/4	0.3882(2)	1.55(9)
Bi(8)/K(3)[b]	1.2936(4)	−1/4	0.3281(6)	4.2(2)
Se(1)	0.9829(5)	−1/4	0.4039(6)	1.7(3)
Se(2)	0.8981(5)	1/4	0.2264(6)	1.5(2)
Se(3)	0.8058(5)	−1/4	0.0596(7)	1.9(2)
Se(4)	0.3885(5)	−3/4	0.2773(7)	2.1(3)
Se(5)	0.8098(5)	−1/4	0.5582(7)	2.1(3)
Se(6)	0.7709(4)	−3/4	0.3711(6)	1.5(2)
Se(7)	0.9570(5)	1/4	−0.0924(6)	1.3(2)
Se(8)	1.1334(5)	−3/4	0.2660(6)	1.6(2)
Se(9)	1.3664(5)	−1/4	−0.1639(6)	1.8(3)
Se(10)	1.4261(4)	−3/4	0.0106(6)	1.3(2)
Se(11)	0.5764(5)	−1/4	0.3224(6)	1.4(2)
Se(12)	1.2776(4)	−1/4	0.1493(7)	1.9(3)
Se(13)	0.6077(5)	−3/4	0.5358(6)	1.5(2)
K(1)/Bi(9)[c]	0.2677(6)	1/4	0.7898(8)	4.8(3)
K(2)	0.510(2)	1/4	0.844(2)	4.6(6)

[a] Anisotropically refined atoms are given in the form of the isotropic equivalent displacement parameter defined as $B_{eq} = (8\pi^2/3)[a^2B_{11} + b^2B_{22} + c^2B_{33} + ab(\cos\gamma)B_{12} + ac(\cos\beta)B_{13} + bc(\cos\alpha)B_{23}]$. The anisotropic temperature factor expression is $\exp[-2\pi^2(B_{11}a^{*2}h^2 + ... + 2B_{12}a^*b^*hk + ...)]$. [b] This site contains 62% Bi and 38% K. [c] This site contains 62% K and 38% Bi.

Table 3. Fractional Atomic Coordinates and Equivalent Atomic Displacement Parameter (B_{eq}) Values for $K_{2.5}Bi_{8.5}Se_{14}$ with Estimated Standard Deviations in Parentheses

atom	*x*	*y*	*z*	B_{eq},[a] Å^2
Bi(1)	0.0932(2)	−3/4	0.4877(2)	1.5(2)
Bi(2)	0.2800(2)	−1/4	0.4364(2)	2.2(2)
Bi(3)	0.4769(2)	−3/4	0.4084(2)	1.5(2)
Bi(4)	0.6607(2)	−1/4	0.3573(2)	1.8(2)
Bi(5)/K(1)[a]	0.8274(8)	1/4	0.2917(8)	2.8(3)
Bi(6)	0.0828(2)	−3/4	0.2304(2)	1.8(2)
Bi(7)[b]	0.3509(8)	−1/4	0.1881(7)	0.7(2)
Bi(8)	0.8749(2)	−1/4	0.1144(2)	1.3(2)
Bi(9)	0.8888(2)	−3/4	0.9279(2)	1.3(2)
Bi(10)	0.6636(2)	1/4	0.9813(2)	1.5(2)
Se(1)	0.4007(5)	−3/4	0.5148(5)	1.0(4)
Se(2)	0.2117(6)	−1/4	0.5592(7)	2.3(5)
Se(3)	0.0176(5)	−3/4	0.5833	1.5(4)
Se(4)	0.1676(6)	−3/4	0.3729(5)	1.7(5)
Se(5)	0.3666(6)	−1/4	0.3423(5)	1.4(4)
Se(6)	0.5462(6)	−3/4	0.3026(5)	1.5(4)
Se(7)	0.7132(7)	−1/4	0.2524(7)	2.5(5)
Se(8)	0.9713(6)	−1/4	0.2440(5)	1.3(4)
Se(9)	0.8108(5)	−3/4	0.7933(6)	1.5(4)
Se(10)	0.5690(6)	1/4	0.8486(6)	1.9(5)
Se(11)	0.7802(5)	1/4	0.1350(6)	1.5(4)
Se(12)	0.9939(6)	−3/4	0.0848(6)	1.3(4)
Se(13)	0.7850(6)	−1/4	0.9484(6)	2.0(5)
Se(14)	0.4219(6)	1/4	0.9888(6)	1.4(4)
K(2)	0.577(1)	1/4	0.145(2)	3(1)
K(3)[b]	0.6667	−1/4	0.796(2)	3(1)

[a] This site contains 24% Bi and 76% K. [b] Bi(7) and K(3) are positionally disordered (30/70%).

Table 4. Fractional Atomic Coordinates and Equivalent Atomic Displacement Parameter (B_{eq}) Values for $K_{2.5}Sb_{8.5}Se_{14}$ with Estimated Standard Deviations in Parentheses

atom	*x*	*y*	*z*	B_{eq},[a] Å^2
Sb(1)	0.0882(2)	−3/4	0.4904(3)	2.9(2)
Sb(2)	0.2796(2)	−1/4	0.4323(3)	2.6(2)
Sb(3)	0.4725(2)	−3/4	0.4099(3)	2.9(2)
Sb(4)	0.6585(1)	−1/4	0.3586(2)	1.2(2)
Sb(5)[a]	0.814(1)	1/4	0.276(2)	0.8(2)
Sb(6)	0.0807(2)	−3/4	0.2249(3)	1.9(2)
Sb(7)[b]	0.6348(4)	−1/4	0.8071(5)	1.2(2)
Sb(8)	0.8754(1)	−1/4	0.1178	0.8(1)
Sb(9)	0.8877(2)	−3/4	0.9280(2)	1.1(2)
Sb(10)	0.6689(1)	1/4	0.9817(2)	0.6(1)
Se(1)	0.4040(3)	−3/4	0.5151(3)	1.3(2)
Se(2)[c]	0.2303(8)	−1/4	0.5765(6)	1.4(2)
Se(2′)[c]	0.799(1)	−3/4	0.421(1)	1.4
Se(3)	0.0133(2)	−3/4	0.5833	1.9(3)
Se(4)[d]	0.1711(8)	−3/4	0.3734(8)	1.8(2)
Se(4′)[d]	0.816(2)	−1/4	0.642(2)	1.8
Se(5)	0.3583(2)	−1/4	0.3458(3)	1.7(3)
Se(6)[e]	0.5154(8)	−3/4	0.2952(9)	0.9(2)
Se(6′)[e]	0.4469(7)	−1/4	0.7029(8)	0.9
Se(7)	0.7096(2)	−1/4	0.2545(3)	0.8(2)
Se(8)	0.9704(2)	−1/4	0.2418(3)	0.7(2)
Se(9)	0.8142(2)	−3/4	0.7992(3)	0.6(2)
Se(10)	0.5741(2)	1/4	0.8545(3)	0.7(2)
Se(11)	0.7812(2)	1/4	0.1386(3)	1.0(2)
Se(12)	0.9948(2)	−3/4	0.0884(3)	1.1(2)
Se(13)	0.7857(2)	−1/4	0.9464(3)	1.1(2)
Se(14)	0.4173(2)	1/4	0.9928(3)	0.8(2)
K(1)[a]	0.8102(7)	1/4	0.298(1)	0.8
K(2)	0.5807(5)	1/4	0.1401(7)	1.1(5)
K(3)[b]	0.664(1)	−1/4	0.783(2)	1.2

These sites are positionally disordered at the percentage ratio: [a]Sb(5)/K(1), 16/84; [b]Sb(7)/K(3), 48/52; [c]Se(2)/Se(2′), 62/38; [d]Se(4)/Se(4′), 70/30; [e]Se(6)/Se(6′), 48/52.

Table 5. Selected Distances (Å) in β-$K_2Bi_8Se_{13}$ with Standard Deviations in Parentheses

Bi(1)−Se(2)	2.76(1)	Bi(2)−Se(3)	3.41(0)
Bi(1)−Se(3) × 2	2.909(7)	Bi(2)−Se(7) × 2	3.146(7)
Bi(1)−Se(7)	3.23(1)	Bi(2)−Se(8)	2.72(1)
Bi(1)−Se(7) × 2	3.026(6)	Bi(2)−Se(12) × 2	2.824(6)
Bi(3)−Se(3) × 2	3.222(7)	Bi(4)−Se(1) × 2	2.944(7)
Bi(3)−Se(9)	2.78(1)	Bi(4)−Se(1)	3.08(1)
Bi(3)−Se(10) × 2	2.772(6)	Bi(4)−Se(5) × 2	2.986(9)
Bi(3)−Se(12)	3.22(1)	Bi(4)−Se(6)	2.88(6)
Bi(5)−Se(5)	2.80(1)	Bi(6)−Se(1)	2.86(1)
Bi(5)−Se(6) × 2	2.893(7)	Bi(6)−Se(2) × 2	2.964(7)
Bi(5)−Se(11)	3.14(1)	Bi(6)−Se(7)	3.00(1)
Bi(5)−Se(13) × 2	3.045(8)	Bi(6)−Se(8) × 2	2.965(7)
Bi(7)−Se(4)	2.74(1)	Bi(8)/K(3)−Se(4) × 2	2.843(9)
Bi(7)−Se(11) × 2	2.830(7)	Bi(8)/K(3)−Se(5) × 2	3.49(1)
Bi(7)−Se(13)	3.36(1)	Bi(8)/K(3)−Se(8)	3.678(9)
Bi(7)−Se(13) × 2	3.098(8)	Bi(8)/K(3)−Se(8)	3.681(9)
		Bi(8)/K(3)−Se(12)	3.31(2)
K(1)/Bi(9)−Se(2) × 2	3.59(1)	Bi(8)/K(3)−Se(13)	3.04(1)
K(1)/Bi(9)−Se(3)	3.07(2)		
K(1)/Bi(9)−Se(6) × 2	3.70(1)	K(2)−Se(4) × 2	3.56(2)
K(1)/Bi(9)−Se(9) × 2	2.85(1)	K(2)−Se(9) × 2	3.28(3)
K(1)/Bi(9)−Se(11)	3.44(1)	K(2)−Se(10)	3.42(3)
		K(2)−Se(10) × 2	3.58(3)
		K(2)−Se(11)	3.42(3)
		K(2)−Se(12)	3.71(3)

The first heating step at 530 °C employed in synthesizing $K_{2.5}Bi_{8.5}Se_{14}$ leads to a mixture of microcrystalline $K_{2.5}Bi_{8.5}Se_{14}$ and a black powder. Recrystallization at 750 °C drives this mixture to pure $K_{2.5}Bi_{8.5}Se_{14}$. A long period of thermal exposure of $K_{2.5}Bi_{8.5}Se_{14}$ to over 750 °C, however, converts it to β-$K_2Bi_8Se_{13}$ with a loss of K_2Se, suggesting that $K_{2.5}Bi_{8.5}Se_{14}$ is a kinetically stable phase. During the preparation of pressed pellets of $K_{2.5}Bi_{8.5}Se_{14}$ for conductivity measurements, we found a new phase forming during annealing under vacuum at 600 °C. This phase grows as extremely thin silvery needles on the surface of the pellet and shows a new XRD pattern. SEM/EDS analysis was performed on several crystals of this new phase to give the average

Table 6. Selected Distances (Å) in $K_{2.5}Bi_{8.5}Se_{14}$ with Standard Deviations in Parentheses

Bi(1)−Se(2) × 2	2.991(7)	Bi(2)−Se(1) × 2	3.055(7)
Bi(1)−Se(3)	2.787(9)	Bi(2)−Se(2)	3.23(2)
Bi(1)−Se(3) × 2	2.918(5)	Bi(2)−Se(4) × 2	2.890(7)
Bi(1)−Se(4)	3.14(1)	Bi(2)−Se(5)	2.90(1)
Bi(3)−Se(1)	3.00(1)	Bi(4)−Se(1)	3.26(1)
Bi(3)−Se(1) × 2	3.058(7)	Bi(4)−Se(2) × 2	3.151(8)
Bi(3)−Se(5) × 2	2.886(6)	Bi(4)−Se(6) × 2	2.871(7)
Bi(3)−Se(6)	2.90(1)	Bi(4)−Se(7)	2.70(2)
Bi(5)/K(1)−Se(2)	3.48(2)	Bi(6)−Se(4)	2.91(1)
Bi(5)/K(1)−Se(3) × 2	3.75(1)	Bi(6)−Se(8) × 2	2.952(9)
Bi(5)/K(1)−Se(7) × 2	2.83(1)	Bi(6)−Se(9) × 2	2.966(9)
Bi(5)/K(1)−Se(8) × 2	3.68(2)	Bi(6)−Se(12)	2.98(1)
Bi(5)/K(1)−Se(11)	3.17(2)		
		Bi(8)−Se(8)	2.72(1)
Bi(7)−Se(5) × 2	3.84(2)	Bi(8)−Se(11) × 2	2.806(8)
Bi(7)−Se(6)	3.48(1)	Bi(8)−Se(12) × 2	3.172(9)
Bi(7)−Se(9) × 2	3.66(2)	Bi(8)−Se(13)	3.36(1)
Bi(7)−Se(10) × 2	2.78(1)		
Bi(7)−Se(13)	3.09(2)	Bi(10)−Se(10)	2.76(1)
		Bi(10)−Se(11)	3.24(1)
Bi(9)−Se(9)	2.74(1)	Bi(10)−Se(13) × 2	3.23(1)
Bi(9)−Se(12)	3.24(1)	Bi(10)−Se(14) × 2	2.780(9)
Bi(9)−Se(12) × 2	3.016(9)		
Bi(9)−Se(13) × 2	2.910(9)	K(3)−Se(5) × 2	3.51(4)
		K(3)−Se(6)	3.61(1)
K(2)−Se(6)	3.58(4)	K(3)−Se(9) × 2	3.30(2)
K(2)−Se(7) × 2	3.42(2)	K(3)−Se(10) × 2	3.16(3)
K(2)−Se(10) × 2	3.35(2)	K(3)−Se(13)	3.23(4)
K(2)−Se(14)	3.53(3)	K(3)−Bi(7)	0.54(5)
K(2)−Se(14) × 2	3.56(3)		

ratio of $K_{1.0}Bi_{5.0}Se_{9.0}$. The remaining material in the pellet is a new phase and has a plate morphology with a very strong XRD peak at 12.59 Å. SEM/EDS analysis on crystals of this phase gives an approximate composition of $K_{1.0}Bi_{3.35}Se_{6.33}$. These results suggest that the solid-state chemistry of $K_{2.5}Bi_{8.5}Se_{14}$ is very complex and warrants continued investigation.[27]

In the synthesis of $K_{2.5}Sb_{8.5}Se_{14}$ as well, both temperature and basicity of the flux are critical. The compound can be prepared in pure form only by the molar ratio (1:2:4−6) of K_2Se/Sb/Se below 530 °C. A reaction of the same ratio of K_2Se/Sb/Se at 600 °C gives mixture of $K_{2.5}Sb_{8.5}Se_{14}$ (yield 20%) and $K_2Sb_8Se_{13}$ (yield 80%) which is isostructural with β-$K_2Bi_8Se_{13}$. At higher temperature (>600 °C) $K_2Sb_8Se_{13}$ and an unidentified K/Sb/Se ternary compound become more stable depending on the basicity of the flux. This indicates that phase equilibria exist among these three compounds. Pure $K_2Sb_8Se_{13}$ was obtained by stoichiometric reaction of K_2Se/Sb/Se at 530 °C. DTA measurements showed β-$K_2Bi_8Se_{13}$, $K_{2.5}Bi_{8.5}Se_{14}$, $K_2Sb_8Se_{13}$, and $K_{2.5}Sb_{8.5}Se_{14}$ melt at 672, 692, 466, and 488 °C, respectively.

Structural Description. *β-$K_2Bi_8Se_{13}$.* This compound is isostructural with the corresponding sulfide $K_2Bi_8S_{13}$ which is different from that of α-$K_2Bi_8Se_{13}$. These two structure types represent an example where similar building blocks combine to give compounds with the same stoichiometry but different architecture. α-$K_2Bi_8Se_{13}$ consists of Bi_2Te_3-, CdI_2-, and Sb_2Se_3-type rod fragments. β-$K_2Bi_8Se_{13}$ possesses a three-dimensional structure made up of Bi_2Te_3-, NaCl-, and CdI_2-type infinite rod-shaped blocks. These different types of fragments are common in other bismuth chalcogenides such as $Cs_3Bi_7Se_{12}$[7] and $KBi_{6.33}S_{10}$.[20] The CdI_2-type and Bi_2Te_3-type rods in β-$K_2Bi_8Se_{13}$ are arranged side by side to form layers perpendicular to the *c*-axis. The NaCl-type rod fragments connect the layers to build a 3-D framework with tunnels filled with K^+ cations. The width of the Bi_2Te_3 and the NaCl rods in this structure is three Bi polyhedra, while the width of the CdI_2-type rod is only two Bi polyhedra. The dimensions of these building blocks define the structural characteristics of each structure type in these materials (also see structure of $K_{2.5}M_{8.5}Se_{14}$ (M = Bi, Sb) below). Overall, the structure of β-$K_2Bi_8Se_{13}$ is slightly more dense than that of the α-form, because in the latter 25% of the Bi atoms are found in a trigonal-pyramidal geometry, while in the former all Bi atoms are in an octahedral or higher coordination geometry (see Figure 1). The origin of the structural and property differences (see below) between these two forms lies partly to the ability of the $6s^2$ lone pair of Bi^{3+} to stereochemically express itself.

Interestingly, the structure of β-$K_2Bi_8Se_{13}$ is closely related to that of $Sr_4Bi_6Se_{13}$[9] by replacing two Sr^{2+} atoms with two K^+ atoms and the remaining two Sr^{2+} atoms with two Bi^{3+} atoms. These substitutions are isoelectronic on average and do not require compositional changes in the "Bi_6Se_{13}" part of the compound. Therefore an alternative way of representing this phase is $(K,Bi)_2Bi_6Se_{13}$.

Among the K^+ cations in β-$K_2Bi_8Se_{13}$, K(2) is fully occupied by K^+ while the others, K(1) and K(3), are disordered with Bi(9) and Bi(8), respectively. Those high-coordinate disordered Bi atoms and CdI_2-type channels serve to stitch the fragments together. The Bi(8) site contains 62% Bi and 38% K while the K(1) site contains 62% K and 38% Bi. The same kind of disorder is found in the isostructural sulfide $K_2Bi_8S_{13}$, with the only difference being that in the sulfide the Bi atoms are disordered over three sites of K(1,2,3). Bi(8) has three normal Bi−Se bonds ranging from 2.843(9) to 3.04(1) Å and five longer distances from 3.31(2) to 3.681(9) Å, resulting in a distorted bicapped trigonal prism. The coordination of the K(1) site is very similar to that of the Bi(8) site. The K(1) site also exhibits three bonds ranging from 2.85(1) to 3.07(2) Å and five longer ones ranging from 3.44(1) to 3.70(1) Å. Since Bi^{3+} and K^+ have similar sizes, this similarity in the coordination environments of the Bi(8) and K(1) sites explains the disorder between Bi and K. On the other hand, the coordination environment of the K(2) site is different by being fully occupied. It can be described as a distorted, tricapped trigonal prism with eight Se atoms in the range between 3.28(3)−3.58(3) Å and one Se atom 3.71(3) Å away. The prism is defined by atoms Se(4), Se(9), Se(10) and their symmetry-equivalent atoms, while the capping atoms are Se(10), Se(11), and Se(12). In contrast, the K(2) site in the sulfide analogue $K_2Bi_8S_{13}$ is 20% occupied with Bi, and it is shifted away from the center of this tricapped prismatic site (the distance between K(2)−S(12) is 4.22(1) Å instead of 3.71(3) Å in the selenide, while the rest of the distances are shorter, in the range 2.72(2)−3.66(2) Å). As a result of this shift, the coordination environment of K(2) site is a bicapped trigonal prism. The K−Se distances below 3.0 Å are unusual and presumably a result of averaging over the mixed K/Bi sites.

(26) (a) Lyding, J. W.; Marcy, H. O.; Marks, T. J.; Kannewurf, C. R. *IEEE Trans. Instrum. Meas.* **1988**, *37*, 76−80. (b) Chaikin, P. I.; Kawk, J. F. *Rev. Sci. Instrum.* **1975**, *46*, 218−220.

(27) Chung, D.-Y.; Kanatzidis, M. G., work in progress.

Table 7. Selected Distances (Å) in $K_{2.5}Sb_{8.5}Se_{14}$ with Standard Deviations in Parentheses

Sb(1)−Se(2)/(2′) × 2	3.25(1)/3.01(1)	Sb(2)−Se(1) × 2	3.062(5)
Sb(1)−Se(3)	2.697(7)	Sb(2)−Se(2)	3.44(2)
Sb(1)−Se(3) × 2	2.807(3)	Sb(2)−Se(4)/(4′) × 2	2.773(8)/2.77(2)
Sb(1)−Se(4)	3.26(2)	Sb(2)−Se(5)	2.624(9)
Sb(3)−Se(1)	2.86(1)	Sb(4)−Se(1)	3.209(8)
Sb(3)−Se(1) × 2	3.001(4)	Sb(4)−Se(2)/(2′) × 2	2.828(8)/3.12(1)
Sb(3)−Se(5) × 2	2.852(4)	Sb(4)−Se(6)/(6′) × 2	3.144(9)/2.760(8)
Sb(3)−Se(6)/(6′)	2.78(2)/3.15(2)	Sb(4)−Se(7)	2.642(7)
Sb(5)−Se(2)/(2′)	3.48(4)/3.19(5)	Sb(6)−Se(4)/(4′)	3.03(2)/2.80(4)
Sb(5)−Se(7) × 2	2.66(1)	Sb(6)−Se(8) × 2	2.893(5)
Sb(5)−Se(8) × 2	3.64(2)	Sb(6)−Se(9) × 2	2.887(5)
Sb(5)−Se(11)	2.78(4)	Sb(6)−Se(12)	2.791(8)
Sb(7)−Se(5) × 2	3.88(1)	Sb(8)−Se(8)	2.606(5)
Sb(7)−Se(6)/(6′)	2.78(1)/3.27(1)	Sb(8)−Se(11) × 2	2.734(4)
Sb(7)−Se(9) × 2	3.758(7)	Sb(8)−Se(12) × 2	3.108(4)
Sb(7)−Se(10) × 2	2.642(7)	Sb(8)−Se(13)	3.460(6)
Sb(7)−Se(13)	3.234(9)		
Sb(9)−Se(9)	2.613(6)	Sb(10)−Se(10)	2.660(6)
Sb(9)−Se(12)	3.301(7)	Sb(10)−Se(11)	3.260(6)
Sb(9)−Se(12) × 2	2.978(4)	Sb(10)−Se(13) × 2	3.130(5)
Sb(9)−Se(13) × 2	2.805(4)	Sb(10)−Se(14) × 2	2.685(4)
K(1)−Se(2)/(2′)	2.98(3)/2.70(3)	K(2)−Se(6)/(6′)	3.83(2)/3.53(2)
K(1)−Se(7) × 2	2.640(8)	K(2)−Se(7) × 2	3.385(9)
K(1)−Se(8) × 2	3.92(2)	K(2)−Se(10) × 2	3.394(9)
K(1)−Se(11)	3.25(2)	K(2)−Se(11)	3.47(1)
		K(2)−Se(14)	3.45(1)
K(3)−Se(5) × 2	3.34(3)	K(2)−Se(14) × 2	3.50(1)
K(3)−Se(6)/(6′)	2.93(2)/3.50(2)		
K(3)−Se(9) × 2	3.27(2)	Sb(5)−K(1)	0.50(5)
K(3)−Se(10) × 2	3.20(3)	Sb(7)−K(3)	0.84(3)
K(3)−Se(13)	3.44(3)	Se(2)−Se(2′)	0.53(3)
		Se(4)−Se(4′)	0.45(5)
		Se(6)−Se(6′)	0.64(2)

Table 8. Selected Angles (deg) in β-$K_2Bi_8Se_{13}$ with Standard Deviations in Parentheses

Se(2)−Bi(1)−Se(3)	91.2(3)	Se(3)−Bi(2)−Se(7)	84.3(3)
Se(2)−Bi(1)−Se(7)	91.0(3)	Se(3)−Bi(2)−Se(9)	87.4(3)
Se(3)−Bi(1)−Se(7)	89.7(2)	Se(3)−Bi(2)−Se(10)	89.9(2)
Se(7)−Bi(1)−Se(7)	86.1(3)	Se(3)−Bi(2)−Se(12)	91.5(3)
Se(3)−Bi(3)−Se(9)	87.4(3)	Se(1)−Bi(4)−Se(1)	87.4(3)
Se(3)−Bi(3)−Se(10)	89.9(2)	Se(1)−Bi(4)−Se(5)	89.5(2)
Se(3)−Bi(3)−Se(12)	91.5(3)	Se(5)−Bi(4)−Se(5)	89.5(3)
Se(9)−Bi(3)−Se(10)	91.6(3)	Se(5)−Bi(4)−Se(6)	88.5(3)
Se(5)−Bi(5)−Se(6)	91.9(3)	Se(1)−Bi(6)−Se(2)	91.2(3)
Se(5)−Bi(5)−Se(13)	89.8(3)	Se(1)−Bi(6)−Se(8)	93.4(3)
Se(6)−Bi(5)−Se(11)	85.3(2)	Se(2)−Bi(6)−Se(7)	87.7(2)
Se(6)−Bi(5)−Se(13)	89.7(2)	Se(7)−Bi(6)−Se(8)	87.8(3)
Se(4)−Bi(7)−Se(11)	91.3(3)	Se(4)−Bi(8)−Se(5)	93.5(2)
Se(4)−Bi(7)−Se(13)	87.3(3)	Se(4)−Bi(8)−Se(8)	85.4(2)
Se(11)−Bi(7)−Se(11)	96.0(3)	Se(4)−Bi(8)−Se(12)	73.4(3)
Se(11)−Bi(7)−Se(13)	92.7(3)	Se(4)−Bi(8)−Se(13)	86.8(3)

Table 9. Selected Angles (deg) in $K_{2.5}Bi_{8.5}Se_{14}$ with Standard Deviations in Parentheses

Se(2)−Bi(1)−Se(3)	92.6(3)	Se(1)−Bi(2)−Se(4)	89.7(2)
Se(2)−Bi(1)−Se(4)	90.0(3)	Se(1)−Bi(2)−Se(5)	87.3(3)
Se(3)−Bi(1)−Se(4)	88.4(2)	Se(4)−Bi(2)−Se(5)	96.2(3)
Se(1)−Bi(3)−Se(5)	88.6(3)	Se(2)−Bi(4)−Se(6)	90.4(2)
Se(1)−Bi(3)−Se(6)	91.0(3)	Se(2)−Bi(4)−Se(7)	95.5(3)
Se(5)−Bi(3)−Se(6)	90.3(3)	Se(6)−Bi(4)−Se(7)	92.8(4)
Se(2)−Bi(5)−Se(7)	86.2(5)	Se(4)−Bi(6)−Se(9)	92.9(3)
Se(7)−Bi(5)−Se(7)	96.0(5)	Se(8)−Bi(6)−Se(9)	89.3(2)
Se(7)−Bi(5)−Se(11)	77.3(4)	Se(9)−Bi(6)−Se(12)	87.7(3)
Se(6)−Bi(7)−Se(10)	74.2(4)	Se(8)−Bi(8)−Se(11)	92.1(3)
Se(10)−Bi(7)−Se(10)	98.1(7)	Se(8)−Bi(8)−Se(12)	88.8(3)
Se(10)−Bi(7)−Se(13)	92.0(4)	Se(11)−Bi(8)−Se(12)	89.9(2)
Se(9)−Bi(9)−Se(12)	91.2(3)	Se(10)−Bi(10)−Se(13)	89.3(3)
Se(9)−Bi(9)−Se(13)	92.4(3)	Se(10)−Bi(10)−Se(14)	93.0(3)
Se(12)−Bi(9)−Se(13)	90.6(3)	Se(11)−Bi(10)−Se(14)	88.4(3)

Bi(4) and Bi(6) possess regular octahedral coordination with Bi−Se bond distances shorter than 3.2 Å which lies well within a single covalent Bi−Se bond.

Table 10. Selected Angles (deg) in $K_{2.5}Sb_{8.5}Se_{14}$ with Standard Deviations in Parentheses

Se(2)−Sb(1)−Se(3)	92.4(3)	Se(1)−Sb(2)−Se(4)	90.6(2)
Se(2)−Sb(1)−Se(4)	89.4(3)	Se(1)−Sb(2)−Se(5)	88.6(2)
Se(3)−Sb(1)−Se(4)	85.6(2)	Se(4)−Sb(2)−Se(5)	96.5(4)
Se(1)−Sb(3)−Se(5)	88.6(2)	Se(2)−Sb(4)−Se(6)	93.0(2)
Se(1)−Sb(3)−Se(6)	96.8(3)	Se(2)−Sb(4)−Se(7)	92.8(3)
Se(5)−Sb(3)−Se(6)	85.6(3)	Se(6)−Sb(4)−Se(7)	94.2(4)
Se(2)−Sb(5)−Se(7)	79.2(9)	Se(4)−Sb(6)−Se(9)	92.8(2)
Se(7)−Sb(5)−Se(7)	100.1(7)	Se(8)−Sb(6)−Se(9)	90.13(9)
Se(7)−Sb(5)−Se(11)	86.1(8)	Se(9)−Sb(6)−Se(12)	87.9(2)
Se(6)−Sb(7)−Se(10)	85.1(3)	Se(8)−Sb(8)−Se(11)	92.6(1)
Se(10)−Sb(7)−Se(10)	101.1(4)	Se(8)−Sb(8)−Se(12)	88.1(1)
Se(10)−Sb(7)−Se(13)	87.2(2)	Se(11)−Sb(8)−Se(12)	90.7(1)
Se(9)−Sb(9)−Se(12)	89.4(2)	Se(10)−Sb(10)−Se(13)	89.1(2)
Se(9)−Sb(9)−Se(13)	92.1(1)	Se(10)−Sb(10)−Se(14)	90.6(1)
Se(12)−Sb(9)−Se(13)	90.1(1)	Se(11)−Sb(10)−Se(14)	88.5(1)

Bi(1), Bi(2), Bi(3), Bi(5), and Bi(7) have a distorted octahedral coordination where a short bond is trans to a long bond while the angles remain close to those of a normal octahedron. For example, the Bi(7)−Se(4) bond distance of 2.74(1) Å is trans to a long Bi(7)−Se(13) distance at 3.36(1) Å. This type of coordination environment is very prevalent in bismuth chalcogenide chemistry and results from the influence of the nonbonded, stereochemically active $6s^2$ electron pair.[20]

$K_{2.5}Bi_{8.5}Se_{14}$ and $K_{2.5}Sb_{8.5}Se_{14}$. These compounds are isostructural to each other and also possess a complex 3D anionic framework which is very similar to that of β-$K_2Bi_8Se_{13}$. Compositionally, $K_{2.5}Bi_{8.5}Se_{14}$ derives from β-$K_2Bi_8Se_{13}$ by addition of 0.5 equiv of $KBiSe_2$. The main difference between the two structures is that in $K_{2.5}Bi_{8.5}Se_{14}$ only NaCl- and Bi_2Te_3-type blocks exist. The latter form by addition of half "$BiSe_2$" atoms to CdI_2-type fragment in β-$K_2Bi_8Se_{13}$. In other

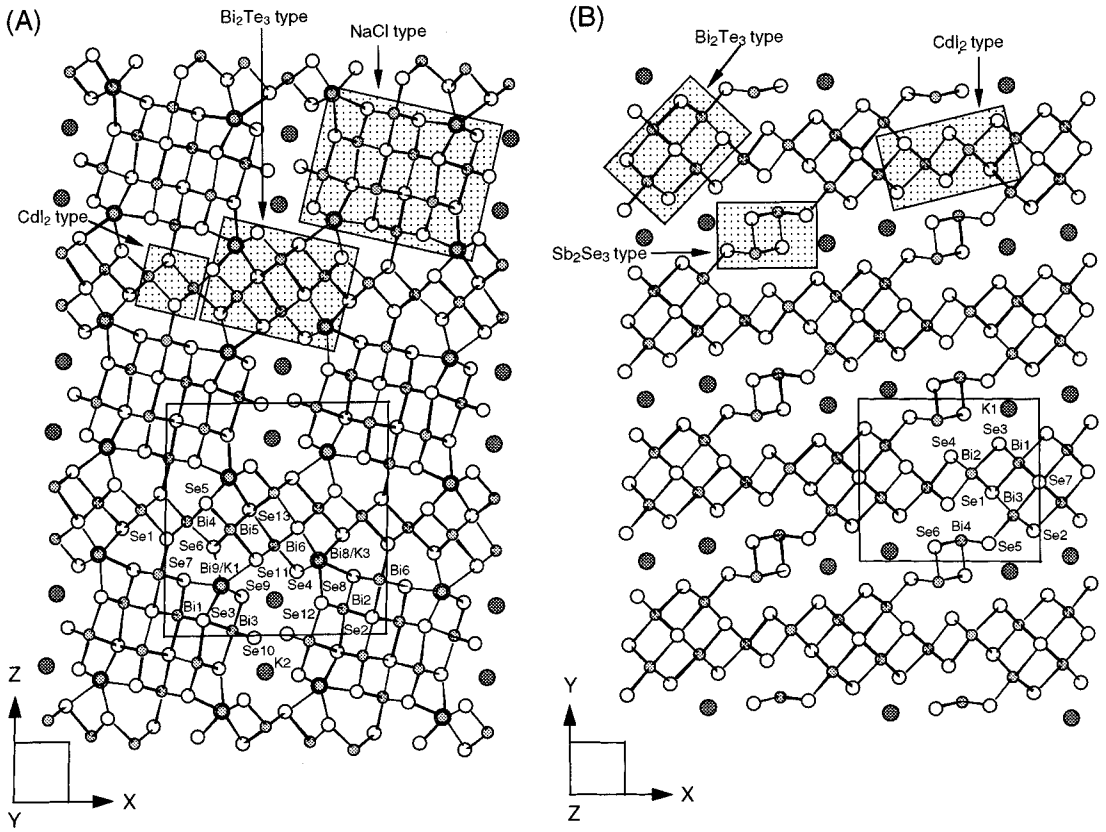

Figure 1. (A) Projection of the structure of β-$K_2Bi_8Se_{13}$ viewed down the *b*-axis. NaCl-, Bi_2Te_3-, and CdI_2-type fragments are found in this framework are highlighted by the shaded areas. (B) Projection of the structure of α-$K_2Bi_8Se_{13}$ viewed down the *b*-axis. Sb_2Se_3-, Bi_2Te_3-, and CdI_2-type building block in the structure are highlighted by the shaded areas.

words, the addition of "$BiSe_2$" in the CdI_2-type blocks of β-$K_2Bi_8Se_{13}$ generates Bi_2Te_3-type blocks which are five-bismuth atoms wide. This small structural modification ingeniously preserves the same connectivity of the NaCl-type fragments and the same size and shape of the K(2) site as in β-$K_2Bi_8Se_{13}$. Although the width of the NaCl block in the structure of $K_{2.5}Bi_{8.5}Se_{14}$ is also three Bi polyhedra, the width of its Bi_2Te_3 block is five Bi polyhedra which is an important difference with the structure of β-$K_2Bi_8Se_{13}$ (see Figure 2).

Atom K(2) in $K_{2.5}Bi_{8.5}Se_{14}$ is fully occupied while K(1) and K(3) are disordered with Bi(5) and Bi(7) at a ratio of 80/20 and 70/30, respectively. K(1) and Bi(5) are located at the same site, which has bicapped trigonal prismatic coordination by Se(2), Se(3), Se(3)′, Se(8), and Se(8)′ with distances ranging from 3.48(2) to 3.75(1) Å and by Se(7), Se(7)′, and Se(11) from 2.83(1) to 3.17(2) Å (the atoms primed outside parentheses are the symmetrically equivalent ones). K(3) and Bi(7) are positionally disordered at the distance of 0.54 Å from each other and K(3) is also surrounded by a bicapped trigonal prism of Se atoms with distances of 3.16(3)−3.61(1) Å. Bi(7) has three short distances (2.78(1)−3.09(2) Å) and five long ones (3.48(1)−3.84(2) Å), the latter being less than the sum (4.23 Å) of van der Waals radii of Bi and Se.

The isostructural analogue, $K_{2.5}Sb_{8.5}Se_{14}$, also has positional disorder in both K(1) and K(3) sites with Sb(5) and Sb(7) at ratios of 84/16 and 52/48. The distances between K(1) and Sb(5) is 0.50(5) Å, and the distance between K(3) and Sb(7) is 0.84(3) Å. In $K_{2.5}Sb_{8.5}Se_{14}$ there is additional disorder in some Se atoms which do not sit exactly on the crystallographic mirror plane, Se(2)/Se(2′) = 62/38, Se(4)/Se(4′) = 70/30, and Se(6)/Se(6′) = 48/52. The Se−Se distance in each pair is 0.53(3), 0.45(5), and 0.64(2) Å, respectively. This Se atom disorder is attributed to a weak 2-fold supercell along *a*-axis (see the solution of this structure).

A characteristic feature in the K−Bi−Q and K−Sb−Q materials is that whenever high coordination sites are found in the lattice (i.e., >6) K/Bi and K/Sb disorder is encountered. This is attributed to the similar ionic sizes of K^+ and Bi^{3+} or Sb^{3+} in high coordination. In octahedral lattice sites, K^+/Bi^{3+} or K^+/Sb^{3+} disorder is less common.

Charge-Transport Properties. The electrical properties of β-$K_2Bi_8Se_{13}$ and $K_{2.5}Bi_{8.5}Se_{14}$ were measured from single-crystal samples and polycrystalline ingots. There is typically a variation of conductivity among crystals of the same compound which may be due to a number of factors including errors associated with measuring the cross-sectional areas of the needlelike crystals. The highest room-temperature conductivity value obtained for single crystals of β-$K_2Bi_8Se_{13}$ was 250 S/cm with a weak negative temperature dependence consistent with a semimetal or a narrow-bandgap semiconducting material (see Figure 3). There is a striking difference in conductivity when comparing to α-$K_2Bi_8Se_{13}$ which shows a room temperature value of 2 S/cm. This is presumably due to the substantial structural differences between the α- and β-forms. Polycrystalline compactions of these materials show similar trends where at room temperature the α-$K_2Bi_8Se_{13}$ has a conductivity of 0.01 S/cm while β-$K_2Bi_8Se_{13}$ and $K_{2.5}Bi_{8.5}Se_{14}$ show ~30 and ~150 S/cm, respectively. This enormous difference is attributed to the fact that

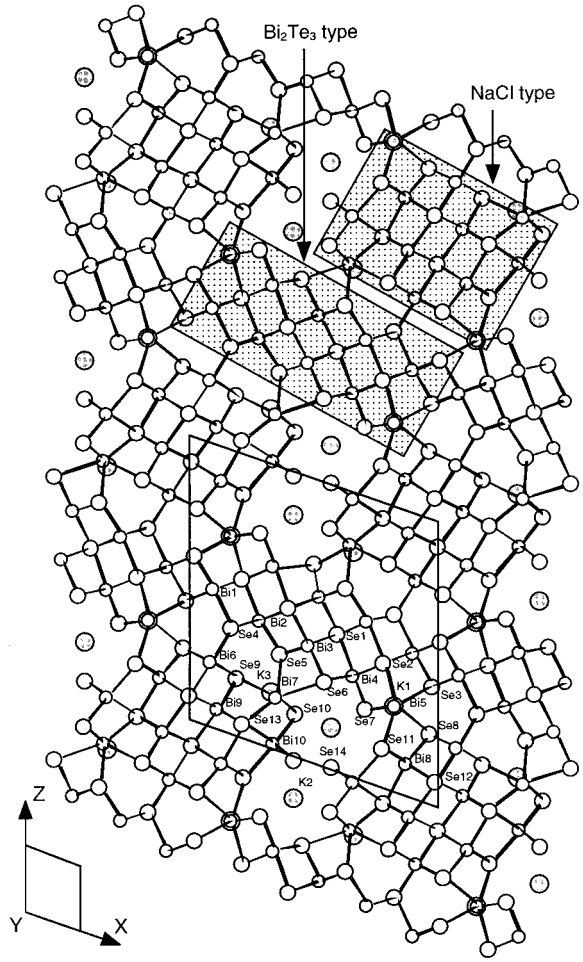

Figure 2. Structure of $K_{2.5}Bi_{8.5}Se_{14}$ projected down the *b*-axis. The isostructural compound $K_{2.5}Sb_{8.5}Se_{14}$ has the same atomic labeling.

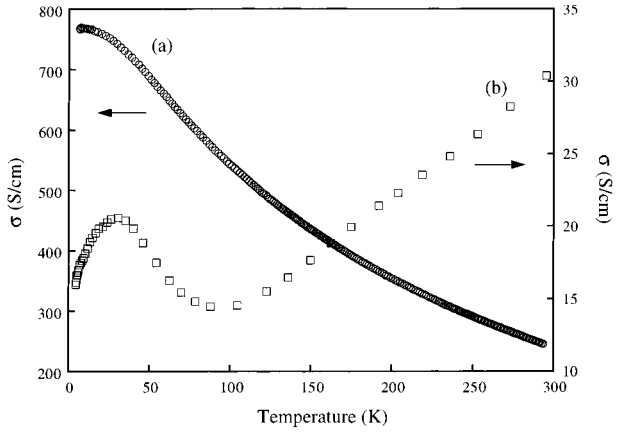

Figure 3. Variable-temperature electrical conductivity data for (a) a single crystal and (b) a polycrystalline ingot of β-$K_2Bi_8Se_{13}$.

β-$K_2Bi_8Se_{13}$ and $K_{2.5}Bi_{8.5}Se_{14}$ have more dense three-dimensional structures than does α-$K_2Bi_8Se_{13}$. The Bi−Se bonding is more extensive in the first two compounds, and this gives rise to greater orbital overlap in the Bi−Se network, broader valence and conduction bands, and consequently lower bandgap. Between β-$K_2Bi_8Se_{13}$ and $K_2Bi_8S_{13}$ the selenide has a higher electrical conductivity as would be expected.

The nature of the charge carriers in these materials was probed with thermoelectric power measurements as a function of temperature. Seebeck coefficient is

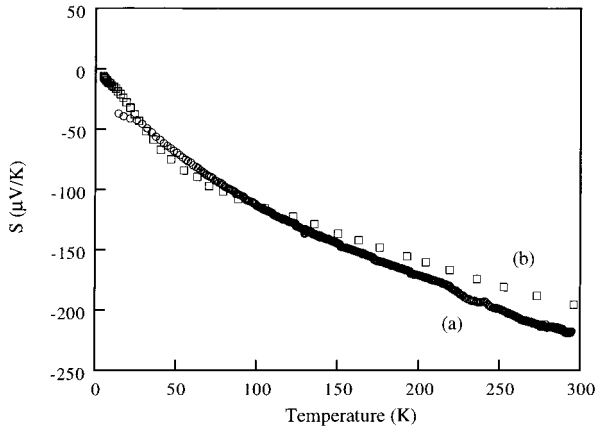

Figure 4. Variable-temperature thermoelectric power data for (a) a single crystal and (b) a polycrystalline ingot of β-$K_2Bi_8Se_{13}$.

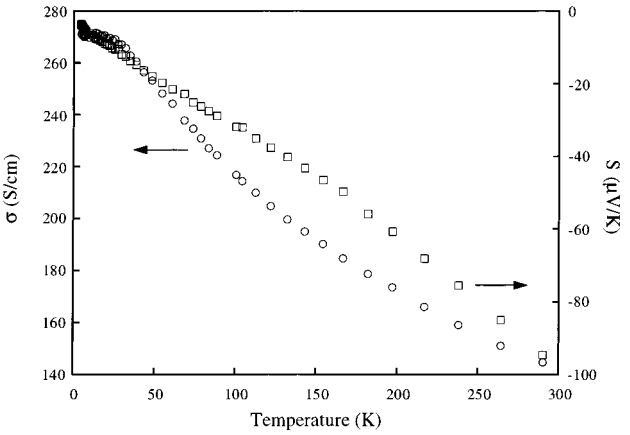

Figure 5. Variable-temperature electrical conductivity and thermoelectric power data for a polycrystalline ingot of $K_{2.5}Bi_{8.5}Se_{14}$.

obtained from the voltage difference across a sample placed in a thermal gradient. It should be noted that such measurements involve no current and are not susceptible to sample morphology (i.e., single crystal vs polycrystalline pellet) and thus probe the inherent properties of the compounds. This is in contrast to the electrical conductivity data which can be dramatically influenced by the existence of grain boundaries.

The thermopower data for β-$K_2Bi_8Se_{13}$ and $K_{2.5}Bi_{8.5}Se_{14}$ show very large negative Seebeck coefficients (−200 and −100 μV/K at room temperature, respectively; see Figures 4 and 5), which indicate the charge carriers are electrons (n-type). It is remarkable that the thermopower behavior and magnitude of the β-$K_2Bi_8Se_{13}$ is similar to that of its α-analogue despite the large differences in conductivity. The thermopower values in these materials become less negative as the temperature is decreased from 300 to 4 K, reminiscent of a metallic behavior, but the very large Seebeck coefficients are more consistent with semiconductors.

Energy Bandgaps. Despite the metal-like temperature dependence of the electrical conductivity and thermopower of β-$K_2Bi_8Se_{13}$ and $K_{2.5}Bi_{8.5}Se_{14}$, the valence precise character indicated by their structure and formulation suggests they should be semiconductors. Indeed, diffuse reflectance spectroscopy on β-$K_2Bi_8Se_{13}$ and $K_{2.5}Bi_{8.5}Se_{14}$ at room temperature revealed the presence of well-defined electronic transitions associated with a bandgap of 0.59 and 0.56 eV, respectively.

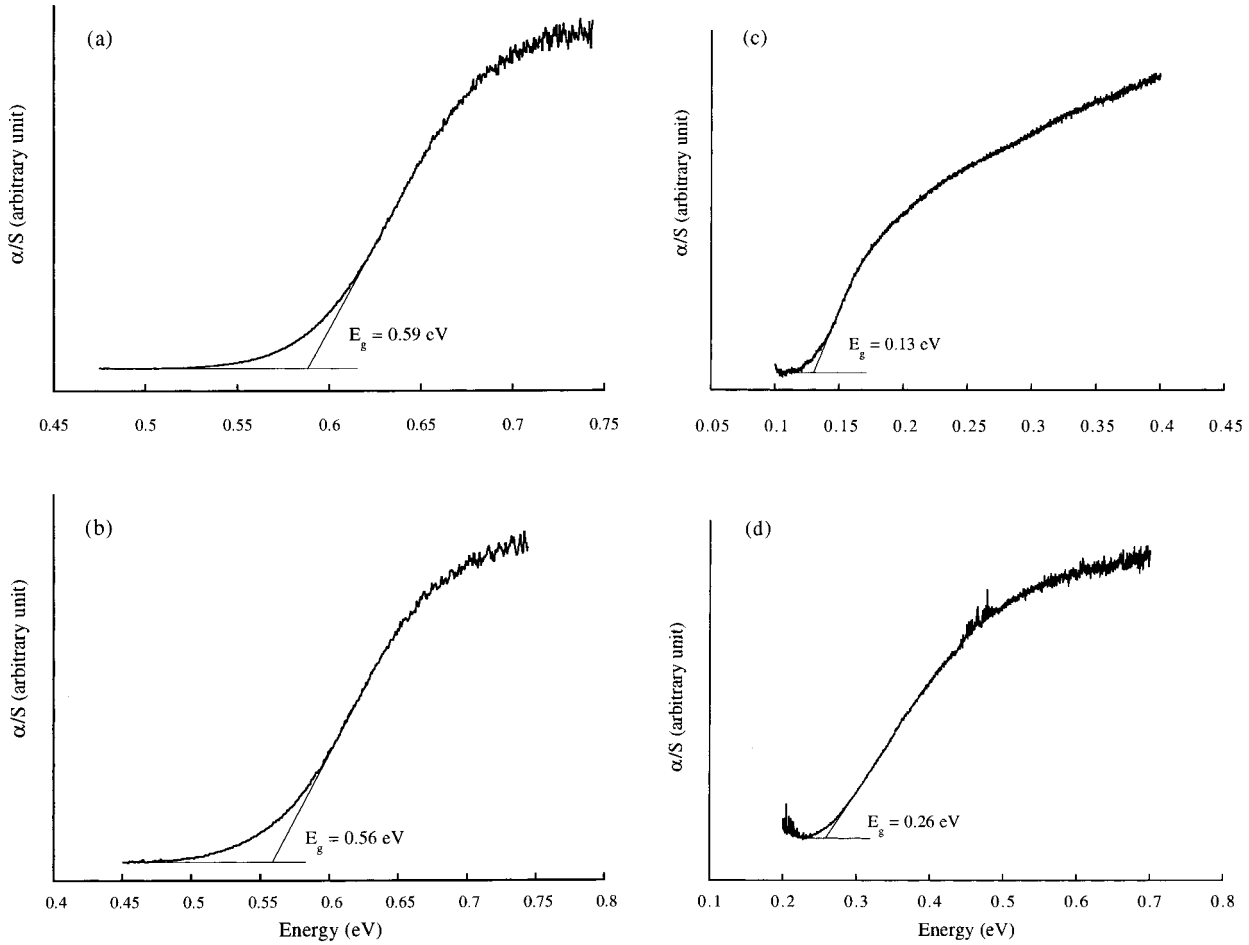

Figure 6. Infrared diffuse reflectance spectra of (a) β-$K_2Bi_8Se_{13}$ and (b) $K_{2.5}Bi_{8.5}Se_{14}$. For comparison, the spectra of (c) Bi_2Te_3 and (d) Bi_2Se_3 are shown. The semiconductor energy gaps are indicated in the spectra.

Diffuse reflectance spectroscopy, in the infrared region, is well suited for the determination of bandgaps in narrow-gap semiconductors, as can be shown by measuring the well-known gaps of Bi_2Te_3 and Bi_2Se_3, see Figure 6c,d.[28,29] At this stage an assessment of the nature of these energy gaps (i.e., direct vs indirect) cannot be made, but the origin of these electronic transitions is thought to be similar to that in Bi_2Se_3, which involves charge transfer from Se p-orbitals to low-lying empty Bi^{3+} orbitals. By comparison, the less dense structure of α-$K_2Bi_8Se_{13}$, which has a slightly more open framework, has a wider gap of 0.76 eV and consequently lower electrical conductivity.

In the case of the Sb analogues, we found greater bandgaps at 0.78 eV for $K_2Sb_8Se_{13}$ and 0.82 eV for $K_{2.5}Sb_{8.5}Se_{14}$ (see Figure 7). This is expected since Sb orbitals have smaller radial extension than Bi orbitals and tend to give rise to narrower bands. Consequently, among isostructural chalcogenide compounds the Sb analogues have higher bandgaps compared to their Bi analogues (e.g., 0.22 eV for Sb_2Te_3 vs 0.13 eV for Bi_2Te_3).

The wider bandgaps of the Sb analogues, $K_2Sb_8Se_{13}$ and $K_{2.5}Sb_{8.5}Se_{14}$, lead to room-temperature conductivities which are 500 times lower than those of the Bi compounds. These low electrical conductivities preclude the Sb analogues from serious consideration as potential thermoelectric materials. Nevertheless, they could be used to prepare solid solutions of the type $K_2Bi_{8-x}Sb_xSe_{13}$ and $K_{2.5}Sb_{8.5-x}Sb_xSe_{14}$.

Annealing Studies. The metal-like behavior of the charge-transport properties of β-$K_2Bi_8Se_{13}$ and $K_{2.5}Bi_{8.5}Se_{14}$ are, therefore, due to heavy doping occurring during synthesis to the point where these materials can be classified as degenerate semiconductors. Such doping could be brought about via slight nonstoichiometry between K/Bi, slight Se deficiency or slight Se excess. The negative thermopower of the materials indicates electrons as the carriers and is consistent with slight Se deficiency. To change the electrical properties of these materials, we carried out annealing experiments under vacuum below the melting point for 36 h, because we expected that this would create additional Se vacancies in the lattice. We found that annealing β-$K_2Bi_8Se_{13}$ in this manner causes the electrical conductivity to rise substantially from ~250 to 670 S/cm at room temperature (see Figure 9). The metal-like slope to the data as a function of temperature is enhanced. At the same time the thermopower decreases from −200 to −100 μV/K (see Figure 9). The negative sign of the thermopower after annealing indicates that the carrier type has not changed. The decrease in magnitude, however, together with the substantial increase in electrical conductivity indicates the number of n-type carriers in the material has increased. This could

(28) Smith, R. A. *Semiconductors*, 2nd ed.; Cambridge University Press: New York, 1978.

(29) The reported bandgaps of Bi_2Te_3 and Bi_2Se_3 are 0.13 and 0.27 eV, respectively. *CRC Handbook of Chemistry and Physics*, 71th ed.; Lide, D. R., Ed.; CRC Press: Boca Raton, FL, 1990; pp 12−62.

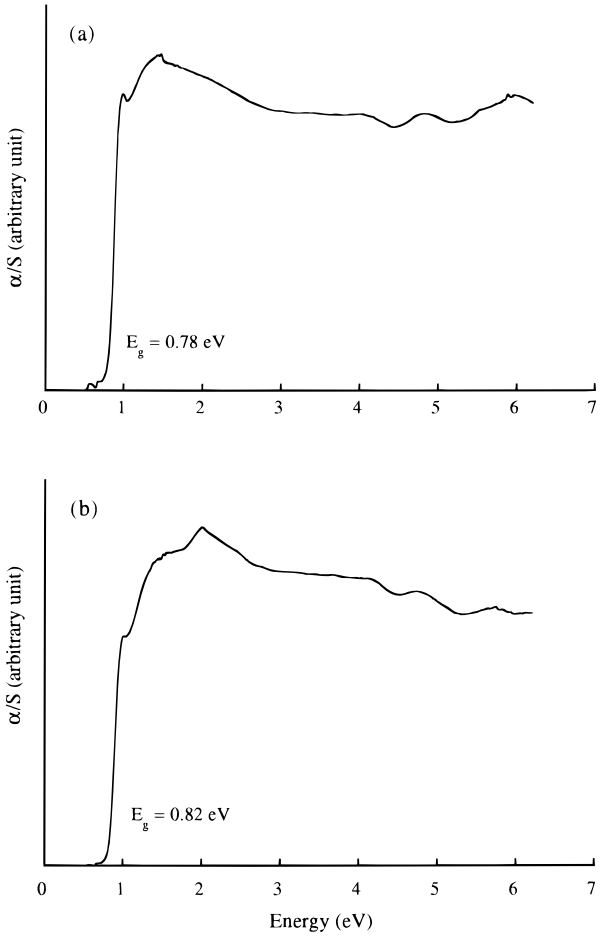

Figure 7. Solid-state UV/vis spectra of (a) $K_2Sb_8Se_{13}$ and (b) $K_{2.5}Sb_{8.5}Se_{14}$.

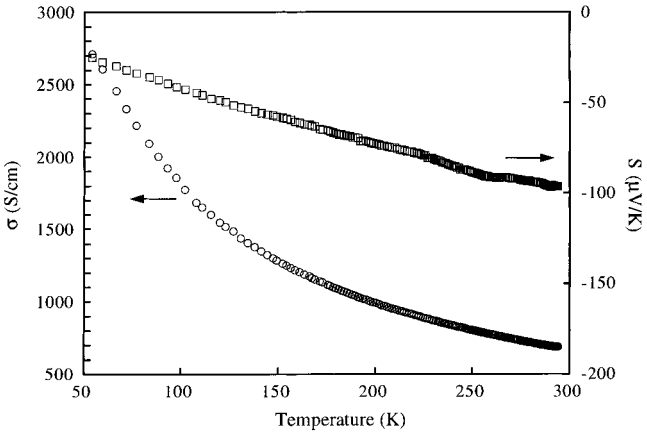

Figure 8. Variable-temperature electrical conductivity and thermopower data for vacuum annealed single-crystal specimens of β-$K_2Bi_8Se_{13}$.

happen through the creation of Se vacancies in the lattice which results in electron injection into the materials conduction band (each Se atom generates two electons).

Single crystals of $K_{2.5}Bi_{8.5}Se_{14}$ were obtained in a reaction of K/Bi/Se at 600 °C as a minor phase which was separated from the major phase β-$KBiSe_2$ and annealed for 3.5 days. These conditions are highly conducive to producing Se-deficient samples in the same way as for β-$K_2Bi_8Se_{13}$ above. In fact, thus far we were able to produce single crystals of $K_{2.5}Bi_{8.5}Se_{14}$ suitable for electrical measurements only under such conditions.

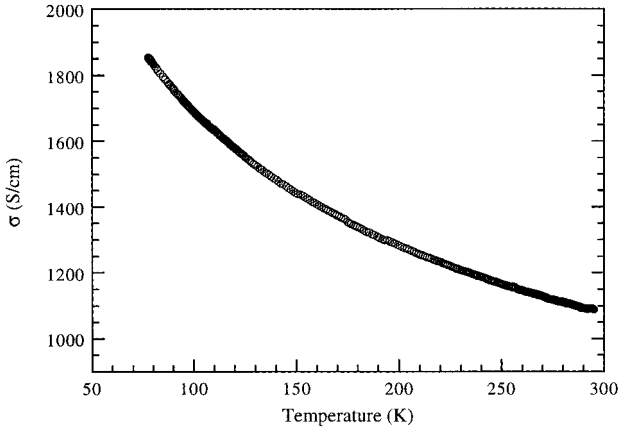

Figure 9. Variable-temperature electrical conductivity for vacuum annealed single-crystal specimen of $K_{2.5}Bi_{8.5}Se_{14}$.

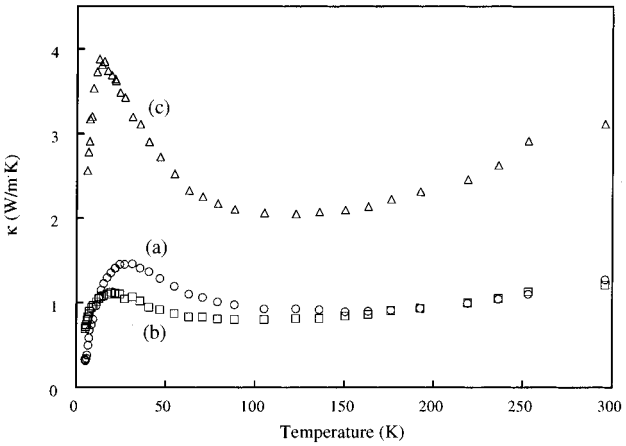

Figure 10. Variable-temperature thermal conductivity data for polycrystalline ingot samples of (a) β-$K_2Bi_8Se_{13}$, (b) $K_{2.5}Bi_{8.5}Se_{14}$, and (c) $K_2Bi_8S_{13}$.

The single-crystal electrical measurements reveal a highly conductive material with a room temperature value of 1100 S/cm and a strong metal-like temperature dependence (see Figure 9). Unfortunately, these crystals are so highly doped that they display an extremely small thermopower at room temperature of -6 μV/K a values typical of metalic materials. We plan to carry out further studies on this material to better understand the thermal effects operating during annealing and to improve its thermoelectric properties.

Thermal Conductivity. The thermal conductivity of a material (κ_T) is the sum of the electronic thermal conductivity (κ_e), due to the electrical carriers (electrons or holes), and the lattice thermal conductivity (κ_l), which is due to the atomic lattice vibrations (phonons). To properly evaluate the potential of β-$K_2Bi_8Se_{13}$ and $K_{2.5}Bi_{8.5}Se_{14}$ for thermoelectric applications, we measured the thermal transport properties of β-$K_2Bi_8Se_{13}$ and $K_{2.5}Bi_{8.5}Se_{14}$ over a wide temperature range (see Figure 10).

The room-temperature thermal conductivities of β-$K_2Bi_8Se_{13}$ and $K_{2.5}Bi_{8.5}Se_{14}$ are comparable (1.28 and 1.21 W/m·K, respectively) and similar to that of optimized Bi_2Te_3 alloy ($\kappa_l \sim 1.3$ W/m·K).[30] This, and work reported earlier,[20] demonstrate that *it is possible to achieve lower thermal conductivity in ternary compounds with complex*

(30) Encyclopedia of Materials Science and Engineering; *Thermoelectric Semiconductors*; MIT Press: Cambridge, MA; Pergamon Press: Oxford, 1986; p 4968.

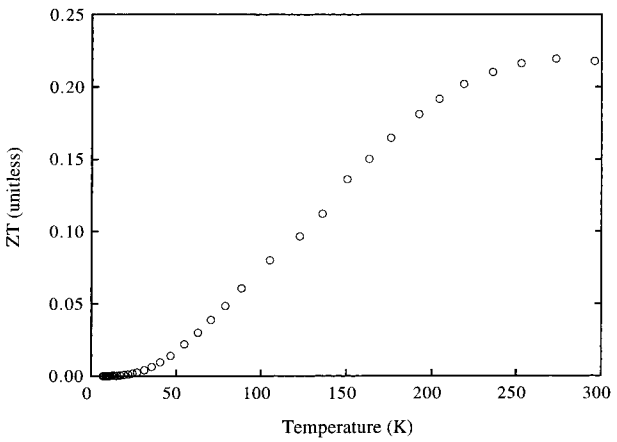

Figure 11. Temperature dependence of the thermoelectric figure of merit (ZT) for β-$K_2Bi_8Se_{13}$.

compositions and crystal structures compared to corresponding high-symmetry binary compounds. Another reason for the very low thermal conductivities of these compounds may be the presence of alkali atoms in tunnels which are only electrostatically interacting with Se atoms on the tunnel walls. This means that these atoms are loosely bound and the fact that the thermal parameters of the K atoms are the largest in the unit cell of both compounds corroborates this. This is in aggreement with Slack's suggestion of an "electron-crystal, phonon-glass"[31] being a key feature of a thermoelectric material. According to this idea loosely bound atoms with large thermal parameters scatter phonons much more strongly than electrons so that they create a glasslike thermal conductivity whithout affecting the electronic mobility which is associated with the covalently bound part of the strucutre, that is the $[Bi_xSe_y]^{n-}$ framework.

Using the measured values of the electrical resistivity in conjunction with the Wiedemann−Franz law,[32] the maximum possible values of the κ_e contribution in both cases were estimated to be less than 10% of κ_T. Thus, essentially all heat in β-$K_2Bi_8Se_{13}$ and $K_{2.5}Bi_{8.5}Se_{14}$ is carried by lattice phonons. The thermal conductivity of β-$K_2Bi_8Se_{13}$ in the temperature range 4−300 K is significantly lower than that of the isostructural compound $K_2Bi_8S_{13}$, which is consistent with the fact that the heavier Se atoms soften the lattice phonons thereby suppressing heat transport in the material.

On the basis of the results presented above, the compound β-$K_2Bi_8Se_{13}$ and $K_{2.5}Bi_{8.5}Se_{14}$ are promising as a thermoelectric materials. The figure of merit (ZT) as a function of temperature for "as-prepared" β-$K_2Bi_8Se_{13}$ is shown in Figure 11. The room-temperature ZT value is 0.22. By comparison *optimized* Bi_2Te_3 has a ZT of 0.87.[33] Given that the compounds reported here have not been optimized, it may be more fair to compare the ZT of β-$K_2Bi_8Se_{13}$ with that of unoptimized (i.e., as prepared) Bi_2Te_3 which is typically in the neighborhood of 0.55. The better performance of Bi_2Te_3 derives mainly from its higher electrical conductivity ($\sigma \sim 850$ S/cm) since the thermopower of the materials reported here is comparable, while their thermal conductivity is equal or lower. A sensible approach to improve the thermoelectric figure of merit of these ternary compounds could be sulfur alloying or solid solutions of $K_xBi_y(Se,S)_z$ and $K_x(Bi,Sb)_y(Se)_z$. This type of alloying is expected to lower the κ_L further and increase the thermopower by increasing energy bandgap.

Concluding Remarks

The reactions of Bi and Sb with K_2Se_x flux have revealed the new compounds, β-$K_2Bi_8Se_{13}$, $K_2Sb_8Se_{13}$, $K_{2.5}Bi_{8.5}Se_{14}$, and $K_{2.5}Sb_{8.5}Se_{14}$. The first two are isostructural with $K_2Bi_8S_{13}$,[20] while the latter two have a different structure type. The A/M/Q (A = alkali metal; M = Sb, Bi; Q = S, Se, Te) system has been found to have a very rich chemistry with compositional and structural varieties of $(A_2Q)_n(M_2Q_3)_m$. As prepared, β-$K_2Bi_8Se_{13}$ and $K_{2.5}Bi_{8.5}Se_{14}$ are n-type semiconductors with narrow bandgaps of 0.59 and 0.56 eV, respectively, and they possess promising properties for thermoelectric applications. It is noteworthy that β-$K_2Bi_8Se_{13}$ exhibits higher electrical conductivity and lower thermal conductivity (1.28 W/m·K), without any loss of thermoelectric power (−200 μV/K), relative to its isostrucutral analogue $K_2Bi_8S_{13}$ and its allotropic kin α-$K_2Bi_8Se_{13}$. This work shows that high thermopowers and high conductivites are possible in ternary K−B−Se systems. It is also evident that low thermal conductivities in low-symmetry, large unit-cell compounds which contain loosely bound alkali atoms in tunnels are relatively easy to achieve. This suggests that the modification of composition and structure of M_2Q_3 by the introduction of A_2Q_x is a viable approach to search for superior thermoelectric properties. The application of dopants to manipulate the electron density at the Fermi level and to control the conductivity type in these materials is now warranted to maximize ZT. Knowledge of the electronic band structure of the compounds will be useful in gaining some insight into the nature of the bands near the Fermi level.

Acknowledgment. Financial support from the Office of Naval Research (Contract N00014-94-1-0935 for M.G.K. and C.R.K. and N00014-96-1-0181 for C.U.) is gratefully acknowledged. The work made use of the SEM facilities of the Center for Electron Optics at Michigan State University. At NU this work made use of Central Facilities supported by NSF through the Materials Research Center (DMR-96-32472).

Supporting Information Available: Tables of crystallographic data and positional and anisotropic thermal parameters of all atoms and observed and calculated powder patterns for compounds **I**, **III**, and **IV** (72 pages); structure factor tables (24 pages). Ordering information is given on any current masthead page.

CM970397E

(31) Slack, G. A. In *CRC Handbook of Thermoelectrics*; Rowe, D. M., Ed.; CRC Press: Boca Raton, FL, 1995; pp 407−440.
(32) Kittel, C. *Introduction to Solid State Physics*, 6th ed.; John Wiley & Sons, Inc.: New York, 1986; p 150.
(33) Scherrer, H.; Scherrer, S. *CRC Handbook of Thermoelectrics*; Rowe, D. M., Ed.; CRC Press: Boca Raton, FL, 1995; pp 211−237.